Delone clusters and coverings for icosahedral quasicrystals

2001 J. Phys. A: Math. Gen. 34 1885

(http://iopscience.iop.org/0305-4470/34/9/306)

INSTITUTE OF PHYSICS PUBLISHING JOURNAL OF PHYSICS A: MATHEMATICAL AND GENERAL

J. Phys. A: Math. Gen. **34** (2001) 1885–1902 www.iop.org/Journals/ja PII: S0305-4470(01)16420-6

Delone clusters and coverings for icosahedral quasicrystals

Peter Kramer

Institut für Theoretische Physik der Universität, Auf der Morgenstelle 14, D 72076 Tübingen, Germany

Received 9 August 2000, in final form 30 November 2000

Abstract

Canonical tilings of type $(\mathcal{T}, \Lambda)$, $(\mathcal{T}^*, \Lambda)$ for quasicrystals are projected from boundaries of Voronoi or Delone cells in an nD lattice Λ. Delone clusters are taken as projections of Delone cells. In general and for icosahedral tilings $\mathcal{T}^*$, projected from the six-dimensional primitive lattices $\Lambda = P$ and from $D_6 \sim 2F$, the Delone clusters and their filling, covering and fundamental domain properties are analysed by dual tiling and window theory.

PACS number: 6144B

1. Introduction

Quasicrystals show long-range atomic order based on quasiperiodicity. A quasiperiodic structure is successfully described as a section $E_\parallel$ of an n-dimensional space E^n equipped with a lattice Λ. The orthogonal complement $E_\perp$ of the section then provides through the concept of windows the characterization of the quasiperiodic structure. The concept of windows applies to atomic positions and neighbourhoods, to tiles, tilings and their vertex configurations, to inflation rules and to Fourier theory. As an example of the fully developed window technique for icosahedral quasicrystals see the work of Katz and Gratias [9, 10].

Covering provides a recent alternative concept for atomic order in quasicrystals. Here the atomic positions are organized into a few clusters of fixed atomic occupation. The covering clusters encompass patches of tiles and thereby reveal new features of atomic correlations in quasicrystals. By overlap these clusters build the long-range structure. Decagonal clusters were derived by Conway [3] and Gummelt [7] in relation to the 2D Penrose–Robinson pattern. Steinhardt and coworkers [20] implemented these decagonal clusters for decagonal quasicrystals and emphasized relations between clusters and unit cells. Duneau [4] constructed different cluster coverings for the vertices of the octagonal and Penrose tilings and gave windows for them. The structures analysed by these authors are all essentially 2D quasiperiodic, complemented by a 1D periodic structure. More recently Duneau [5] and Gratias *et al* [6] studied extended clusters in icosahedral quasicrystals. Their clusters are required to cover the atomic positions of specific models. Connections between the window and covering

0305-4470/01/091885+18$30.00

approach were given in [15] in particular for the one-dimensional Fibonacci and the two-dimensional Penrose and triangle tilings. All these tilings arise by projection from the dual lattice geometry of the Voronoi and Delone cells. In the same context, V and D clusters were constructed as projections of Voronoi and Delone cells. The notion of fundamental domains was introduced and used to examine the relation between clusters and unit cells. The full lattice geometry and the relation between these notions was elaborated in [17] for the Delone clusters in the triangle tiling and the lattice $\Lambda = A_4$.

In what follows we go beyond the specific tilings analysed so far. We explore Delone clusters, covering and fundamental domains as general concepts in the structure of quasicrystals. In sections 1–6 we introduce general notions and results on lattices, dual cells and boundaries, dual tiling theory and covering for quasicrystals. We demonstrate that these clusters appear and can be constructed with general features in all dual tilings. Since we can keep the relation to the tilings within these clusters, they provide frames of reference for a variety of atomic positions.

In the following sections 7–13 we implement the icosahedral Delone clusters and their windows. We derive unique fillings of these clusters in tilings for the icosahedral lattices $\Lambda = P$ and $D_6 \sim 2F$. The latter appears very often in icosahedral quasicrystals. We examine the fundamental domain and the covering properties and find relations depending on the lattice. The distinction between the covering of quasiperiodic points and of quasiperiodic tiles becomes manifest in these tilings. Main results derived here were announced in [16].

2. Voronoi and Delone cells and dual boundaries

Consider for even n a lattice Λ whose basis spans E^n. We pass from the lattices $\Lambda \subset E^n$ to dual polytopes and by projection form the building blocks for tilings and their windows. The following properties, compare [3, 13], apply to all lattices under consideration. The Voronoi cell at a point $q \in \Lambda$, $\Lambda \subset E^n$ is the set of points $V(q) = \langle x | q' \neq q \rightarrow |x - q| \leqslant |x - q'| \rangle$. It is a convex polytope bounded by hyperplanes. Its p-boundaries of dimension p, $0 \leqslant p \leqslant n$ we denote by $X(q)$ where the argument q keeps track of the centre of the bounded Voronoi domain. The 0-boundaries, the vertices of the Voronoi cells, are the holes, [3, p 33], of the lattice. A p-boundary $X(q)$ will in general bound also other Voronoi domains $V(q')$ with $q' \neq q$.

Definition 1 (Dual boundaries). *For any fixed p-boundary $X(q) \in V(q)$, let $s(X) = \langle q' \rangle$ denote the set of all lattice points q' (including q) which have $X = X(q)$ as a boundary of their Voronoi cell $V(q')$.*

(i) The intersection polytope $Y := \cap_{q' \in s(X)} V(q')$ determines the boundary $X = Y$.
(ii) The boundary X^* dual to X is the polytope defined as the convex hull $X^* := \langle \mathrm{conv}(q'), q' \in s(X) \rangle$.

Boundaries and their duals have complementary dimensions $(p, n-p)$. Given a boundary $X(q)$, the vertices or 0-boundaries $q' \in X^*(q)$ of its dual $X^*(q)$ determine by definition 1 the set $s(X)$, so we may write $s(X) = \langle q' \rangle = s(X^*)$. The duals to the 0-boundaries or holes h are the Delone cells D^h, [3, p 35], of the lattice. These dual Delone cells are bounded by dual $(n-p)$-boundaries X^*. The following general inclusion properties arise [13] from duality:

Proposition 2 (Inclusion relations of dual boundaries). *Consider dual pairs of boundaries X, X^* and Y, Y^*.*

(i) If $X \subset Y$ then $Y^* \subset X^*$,

(ii) if $X^* \subset Y^*$ then $Y \subset X$.

Under the action of Λ, both the holes h and the Delone cells D^h fall into a finite number of distinct orbits which we denote by $h = a, b, \ldots$.

3. Dual tilings and their windows

A decomposition $E^n = E_\parallel + E_\perp$, $\dim(E_\parallel) = \dim(E_\perp) = n/2 =$ integer, irrational with respect to the lattice $\Lambda \subset E^n$, arises in quasicrystals from a non-crystallographic point symmetry. For icosahedral point symmetry compare section 7. It allows us to project boundaries and their duals. From the $(n/2)$-boundaries of Voronoi and Delone cells we define in E^n the klotz polytopes [11, 13] as the direct products

$$\begin{aligned} &X_{j\parallel}(q) \otimes X^*_{j\perp}(q) \\ &X^*_{j\parallel}(q) \otimes X_{j\perp}(q) \end{aligned} \tag{1}$$

where the index j labels different $(n/2)$-boundaries. The next two results were obtained in [13]:

Proposition 3. *The klotz polytopes equation (1) in E^n have the following properties:*

(i) They form a Λ-periodic tiling of E^n,
(ii) any boundary of a klotz polytope is either parallel or perpendicular to the subspaces $E_\parallel$ and $E_\perp$.
(iii) If the set of boundaries $\langle X_j(q)\rangle$ at a fixed lattice point q forms orbit representatives under Λ, then the corresponding set of representative klotz polytopes is a fundamental domain (section 4) with respect to Λ.

Proposition 4 (Canonical tilings). *The cuts $E_\parallel + c_\perp$ through the first or second klotz construction of equation (1) are two tilings $(\mathcal{T}, \Lambda)$, $(\mathcal{T}^*, \Lambda)$. The tiles are projections of the $(n/2)$-boundaries $X_{j\parallel}$ or $X^*_{j\parallel}$ from Voronoi and Delone cells respectively. It suffices to let $c_\perp$ run over the projection of the unit cell in $E_\perp$.*

Turn to the window description of these tilings. A window $w(X^*) \in E_\perp$ is defined as a polytope in E^n such that $X^* \in \mathcal{T}^*$ appears whenever $(E_\parallel + c_\perp) \cap w(X^*) \neq 0$. In this description the windows must be attached to all lattice points.

In what follows we shall consider the tilings $(\mathcal{T}^*, \Lambda)$.

Proposition 5. *The windows for the tiles in the canonical tilings are $w(X_{j\parallel}) = X^*_\perp$, $w(X^*_{j\parallel}) = X_\perp$ respectively. The window for the projected lattice points $q_\parallel$, which in $(\mathcal{T}^*, \Lambda)$ form the vertices of the tiles, is $V_\perp$.*

Proof. The first part follows from the properties of the klotz construction equation (4): the tile $X^*_{j\parallel}$ appears whenever its dual $X_{j\perp} \in V_\perp$ intersects with $E_\parallel + c_\perp$. By use of the dual inclusion relation proposition 2 one finds that all projected lattice points $q_\parallel$ are 0-boundaries of a tile $X^*_{j\parallel}$. The projected dual Voronoi cell $V_\perp$ therefore must contain the tile window $X_{j\perp}$, and this tile window in turn must contain the perpendicular projection $q_\perp = q - q_\parallel$. □

An alternative description of the tilings uses windows only at one fixed lattice point, say $q = 0$. This can be seen as follows. Assume $c_\perp \in V_\perp(0)$. The intersection of tile windows with $c_\perp \cap w(X^*_{j\parallel}) \neq 0$ determines a union of tiles $\cup_j X^*_{j\parallel}$ which share a vertex of $(\mathcal{T}^*, \Lambda)$ and close the solid angle around it. This is a vertex configuration. Each Delone edge or 1-boundary of a tile of $(\mathcal{T}^*, \Lambda)$ in this configuration is the projection $q_\perp$ of a lattice vector $q = q_\parallel + q_\perp$. We can move in the tiling along $q_\parallel = q - q_\perp$ from the initial to a next vertex and refer it to

the new $V_\perp(q)$. This is equivalent to the replacement $c_\perp \to c_\perp - q_\perp$ while keeping the initial window $V_\perp(0)$. We may therefore keep the initial window and its boundaries, transform the value of $c_\perp$ by $-q_\perp$ in the window $V_\perp$ and move by $q_\parallel = q - q_\perp$ from vertex to vertex in the tiling.

4. Fundamental domains

To explore unit cell properties for quasicrystals we need concepts of fundamental domains as particular point sets under the action of translations. We distinguish a geometric action on point sets from an action by linear operators on elements of a linear space of functions. The class of functions we have in mind should in crystals or quasicrystals describe observables such as atomic positions or the electronic charge density. We follow the standard notions given in [15]. For E^n equipped with a lattice Λ we recall the well known

Definition 6. *Consider the geometric action $\Lambda \times E^n \to E^n$ given by $q \in \Lambda, x \in E^n : (q, x) \to x' = x + q$. A fundamental domain $\mathcal{F}$ of E^n under Λ is a subset which has exactly one point from each orbit under this action.*

Definition 7. *Consider complex-valued functions f with domain of definition E^n and define for $q \in \Lambda$ group operators by $T_q : f(x) \to (T_q f)(x) := f(x - q)$. Suppose that f is Λ-periodic. A fundamental domain for f is a subset $\mathcal{F}(\Lambda)$ of points such that any value taken by f on $E^n - \mathcal{F}(\Lambda)$ can be obtained by the group action of Λ on f.*

Both notions yield the same candidates for fundamental domains as cells for the lattice. The shape of the fundamental domain is not unique; the primitive and the Voronoi cell for a lattice are examples of fundamental domains. The volume $V(\mathcal{F})$ is unique.

We need an extension of the notion of a fundamental domain to quasiperiodic systems, in the absence of periodic lattice symmetry. Consider an irrational linear subspace $E_\parallel \subset E^n$. The restriction of a Λ-periodic function f from E^n to the domain $E_\parallel$ of dimension m determines a general quasiperiodic function on $E_\parallel$ (compare Bohr [2] and Arnold [1]). In general the irrational subspace $E_\parallel$ will slice E^n and hit a dense subset of the n-dimensional unit cell modulo Λ. It follows that a reasonable generalization of the fundamental domain for a general quasiperiodic function on m-dimensional $E_\parallel$ is still the n-dimensional fundamental domain $\mathcal{F} = \mathcal{F}(\Lambda)$. In this generality, the fundamental domain is essentially a polytope of dimension n larger than the dimension m of the domain $E_\parallel$ of the quasiperiodic function.

A different concept of fundamental domain applies for a class of quasiperiodic tilings, projected again from a lattice $\Lambda \in E^n$ to a subspace $E_\parallel$ of dimension $m < n$. For this class of quasiperiodic tilings we can require the quasiperiodic functions to be compatible with the tiling. We follow [11] and [15] and extend the notions of definitions 6 and 7 by

Definition 8. *Let a quasiperiodic tiling $(\mathcal{T}, \Lambda)$ consist of a minimal finite set $\langle P_i \rangle$ of prototiles $P_i \in E_\parallel$ and their translates. A fundamental domain $\mathcal{F}(\mathcal{T}, \Lambda)$ is a subset of points in $E_\parallel$ which contains one and only one translate of any point from any prototile.*

Definition 9. *A quasiperiodic function f on $E_\parallel$ is called compatible with the tiling $(\mathcal{T}, \Lambda)$ if its values are repeated on all the translates in $(\mathcal{T}, \Lambda)$ of any prototile. A fundamental domain for such functions is a subset $\mathcal{F}(\mathcal{T}, \Lambda) \subset E_\parallel$ such that any value taken by f on $E_\parallel - \mathcal{F}(\mathcal{T}, \Lambda)$ arises by a translation between tiles in the tiling from an identical value on $\mathcal{F}(\mathcal{T}, \Lambda) \subset E_\parallel$.*

The translation vectors of a prototile in a quasiperiodic tiling all belong to the module $\Lambda_\parallel$. If two translates of a fixed prototile occur in the tiling, the sum of the two translation vectors in

general need not be a translation vector in the tiling for this prototile. The notions definitions 8 and 9 yield the same candidates for fundamental domains. In contrast to general quasiperiodic functions, these fundamental domains can be taken as bounded point sets in $E_\parallel$ of dimension m. One natural choice for them is the set of all points from all the prototiles. The volume of this fundamental domain for this and any other choice can be determined in terms of the prototiles by $|\mathcal{F}(\mathcal{T}, \Lambda)| = \sum_i |P_i| < \infty$.

5. Delone clusters and their windows

We explore the properties of Delone clusters.

Definition 10 (Delone clusters). *A Delone D^h-cluster in the tiling $(\mathcal{T}^*, \Lambda)$ is [15] the parallel projection $D^h_\parallel$ of a Delone cell from the lattice Λ.*

We shall construct the Delone clusters in the tiling from their windows $w(D^h)$.

Proposition 11 (Filling of Delone cell). *Fix a hole point $h_\perp$ in $E_\perp$ and consider all the projected $(n/2)$-boundaries $X_{j\perp}(h)$ (i) each with a vertex h at this hole point. Determine a maximal intersection w of these projected boundaries which (ii) share at least one fixed interior point $x_\perp \neq h_\perp$,*

$$w = \cap_j X_{j\perp}(h). \tag{2}$$

Then $w = w(D^h_\parallel)$ is the window for a Delone cluster $D^h_\parallel$. The Delone cluster is the union of all the projected tiles dual to those occurring in equation (2),

$$D^h_\parallel = \cup_j X^*_{j\parallel}. \tag{3}$$

This union is a filling of $D^h_\parallel$ with no gaps and no overlaps of dimension $(n/2)$, and compatible with the tiling.

Proof. First part: the hole point h by assumption (i) is a 0-boundary contained in any $(n/2)$-boundary $X_j(h)$ of the intersection equation (2), $h \subset X_j(h)$. The dual to this 0-boundary is a Delone cell D^h. With proposition 2 it follows that $X^*_j \subset D^h$. This subset property extends to the projections. Second part: the tile windows for any pair $X_{j\perp}, X_{l\perp}$, $j \neq l$ by assumption (ii) intersect in at least one interior point $x_\perp$. Consider the corresponding klotz polytopes, equation (1), indexed by j, l. Their projections to $E_\perp$ share an interior point. For their projections to $E_\parallel$ we conclude $X^*_{j\parallel} \cap X^*_{l\parallel} = 0$; there is no overlap for $j \neq l$. Otherwise the full nD klotz polytopes would share interior points. □

We now describe the complex relation of the filled Delone cluster to the tiling. In the window description of proposition 11, the intersecting tiles $X_{j\perp}(h)$ which form the window $w(h)$ share the hole position h but belong to Voronoi cells at various lattice points q. These lattice points for each coding tile can be found as follows: go within $E_\perp$ for each coding tile in equation (2) to its dual as $X_{j\perp} \to X^*_{j\perp}$. The vertices of $X^*_{j\perp}$ by definition 1 are projections $q'_\perp$ of all the lattice points q' whose Voronoi cells have X_j as a boundary. To find from equation (2) all vertex configurations which contribute to the filling equation (3), we must collect the full set of lattice points $s(D^h) = \langle q' | q' \in X^*_j, X_{j\perp} \in w(D^h_\parallel)\rangle$. Starting from one such projection $q_\perp \in V_\perp(q)$, an initial window $w(h)$ must belong to $V_\perp(q)$. We shift this initial window to all the positions $\langle w(h) + (q' - q)_\perp\rangle$, $q' \in s(D^h_\parallel)$. All these shifted windows are inside $V_\perp(q)$ and determine parts of the full window for a fixed orientation. In the tiling the set of parallel projections $\langle q'_\parallel, q' \in s(D^h)\rangle$ becomes the complete vertex set from which the filling $D^h_\parallel$ can be seen in the tiling. The shifted windows in $V_\perp(q)$ determine all the vertex configurations

appearing in this filling. The vertex configurations inside the filling are complete, those at the boundary of the filling are incomplete.

The filling $D^h_\parallel$ can occur in various orientations. By application of the point group G at a fixed hole of type h in $V_\perp$ one finds a G-window $w_G := G \times w(h)$. It codes all the orientations of the filling $D^h_\parallel$ seen from a fixed vertex. Repeating this construction at any hole of type h in $V_\perp$ one finds the total window for this type.

All these constructions are exemplified in detail in [17] for Delone clusters in the quasiperiodic triangle tiling.

6. Covering by Delone clusters

Once the windows of the Delone clusters have been constructed, their covering properties can be explored by relating these windows to the windows of the tiling. We distinguish covering of vertices from covering of tiles. From dual tiling theory we give criteria for them.

Proposition 12 (Window criterion for covering of vertex points). *The Delone clusters form a covering of lattice or vertex points $q_\parallel$ in the tiling $(\mathcal{T}^*, \Lambda) \subset E_\parallel$ if and only if the collection $\bigcup_i w_G(D^i_\parallel)(h_{i\perp})$ of all shifted G-windows covers $V_\perp$.*

Proof. If the criterion is fulfilled, any point in a tile window $q_\perp \in X_\perp \subset w(X^*_\parallel)$ is in the window of at least one Delone cluster. It follows that the corresponding point $q_\parallel = (q - q_\perp) \in X^*_\parallel$ is covered by this Delone cluster. The converse works as well. □

Proposition 13 (Window criterion for covering of tiles). *A tile $X^*_\parallel$ in the tiling is covered by at least one Delone cluster if and only if its window $w(X^*_\parallel)$ is covered by all the windows $w(h)$ at the local hole vertices $h_\perp \in X_\perp$.*

Proof. Any hole vertex $h_\perp \in X_\perp$ is (the projection of) an intersection of the $(n/2)$-boundary $X_{j\perp}$ with a 0-boundary of a Voronoi cell. The dual inclusion relation according to proposition 2, section 4, is that $X^*_{j\parallel}$ as a boundary belongs to the Delone cell $D^h_\parallel$. □

The distinction between the coverings according to propositions 12 and 13 is relevant. Clearly the covering of tiles according to proposition 13 implies the covering of lattice points, proposition 12. The converse is not true. It is easy to imagine a full covering of all the vertices in a tiling which does not cover all the points of the tiles. A full covering of all points $x \in E_\parallel$ in a tiling requires that any point of any tile be covered. In the two-dimensional triangle tiling [17] the Delone clusters cover all tiles and therefore all vertices. We shall see in section 13 that in icosahedral tilings this is not the case.

7. Six-dimensional lattices and the icosahedral Coxeter group

We introduce the lattices and point groups used for the construction of icosahedral tilings. By Λ we denote both a lattice and its translation group. The primitive hypercubic lattice $\Lambda = P$ in six dimensions spanned by six orthonormal unit vectors $(e_1, \ldots, e_6)$ we denote as

$$P = \left\langle \sum_j n_j e_j, n \in Z^6 \right\rangle \qquad e_l \cdot e_k = \delta_{lk}. \tag{4}$$

The holohedry of this lattice is the hyperoctahedral group $\Omega(6)$, $|\Omega(6)| = 2^6 6!$, generated by all permutations and reflections of the basis vectors. The standard root lattice $\Lambda = D_6$ [3] can

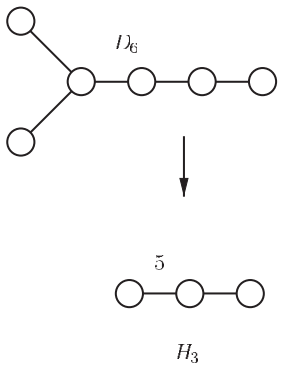

Figure 1. Coxeter diagrams for D_6 and its subgroup H_3.

be taken as a centring $2F$ of P. We keep a factor 2 in order to have simple relations to the lattice P. A basis of $D_6 \sim 2F$ is

$$(b_1, \ldots, b_6) = (e_1, \ldots, e_6)Z^{2F} \tag{5}$$

$$Z^{2F} = \begin{bmatrix} 1 & 0 & 0 & 0 & 0 & 0 \\ 0 & 1 & 0 & 0 & 0 & 0 \\ 0 & 0 & 1 & 0 & 0 & 0 \\ 0 & 0 & 0 & 1 & 0 & 0 \\ 0 & 0 & 0 & 0 & 1 & 0 \\ \overline{1} & \overline{1} & \overline{1} & \overline{1} & \overline{1} & 2 \end{bmatrix}. \tag{6}$$

The Weyl group of D_6 is a Coxeter group which has the icosahedral Coxeter group H_3, $|H_3| = 120$ as a subgroup. We give the Coxeter diagrams for both groups in figure 1.

The Coxeter relations for the generators of H_3 read

$$R_1^2 = R_2^2 = R_3^2 = (R_1R_2)^5 = (R_2R_3)^3 = (R_3R_1)^2 = e. \tag{7}$$

In the lattices these generators can be expressed as signed permutations acting on the basis vectors equation (4),

$$R_1 = (23)(46) \qquad R_2 = (36)(45) \qquad R_3 = (15)(2\overline{3}). \tag{8}$$

The six-dimensional representation of H_3 is reducible into two inequivalent three-dimensional irreducible representations $\mathcal{D}_\parallel(H_3), \mathcal{D}_\perp(H_3)$ in orthogonal subspaces $E_\parallel, E_\perp$. An explicit reduction $H_3 = M^{-1}\mathcal{D}_\parallel(H_3) \oplus \mathcal{D}_\perp(H_3)M$ is provided [12, 14] by the matrix

$$M = \sqrt{1/2(\tau+2)} \begin{bmatrix} 0 & 1 & \overline{1} & \overline{\tau} & 0 & \tau \\ 1 & \tau & \tau & 0 & \overline{1} & 0 \\ \tau & 0 & 0 & 1 & \tau & \overline{1} \\ 0 & \tau & \overline{\tau} & 1 & 0 & \overline{1} \\ \tau & \overline{1} & \overline{1} & 0 & \overline{\tau} & 0 \\ \overline{1} & 0 & 0 & \tau & \overline{1} & \tau \end{bmatrix}. \tag{9}$$

$\mathcal{D}_\parallel(H_3)$ is the standard defining irreducible representation of H_3. The parallel and perpendicular projections of the six unit vectors equation (4) are given by the set of column vectors in the upper and lower three rows of equation (9) respectively. To the three generators, equation (8), there correspond in $E_\parallel$ three Weyl vectors perpendicular to reflection planes,

$$R_1 \to (e_6 - e_4)_\parallel \qquad R_2 \to (e_6 - e_3)_\parallel \qquad R_3 \to (-e_2 - e_3)_\parallel. \tag{10}$$

The stereographic projections of all axes were given in figures 12.2 and 12.3 of [14]. The three reflection planes intersect pairwise in closest five-, three- and twofold axes and bound an

infinite Coxeter cone. The points within this infinite Coxeter cone form a fundamental domain under the action of the Coxeter group on $E_\parallel$. Under $\mathcal{D}_\parallel(H_3)$, all similar Coxeter cones are mapped into one another. By a spherical Coxeter cone we denote the intersection of this infinite cone with the unit sphere in $E_\parallel$. In later sections we shall require intersections of the infinite Coxeter cone with polyhedra centred at the intersection of the reflection planes. In $E_\perp$ the corresponding Weyl reflections are still given by the signed permutations equation (8), which now act on the perpendicular projections of the vectors equation (4). Since the representation $\mathcal{D}_\perp(H_3)$ in $E_\perp$ is inequivalent, the Coxeter cone in $E_\perp$ as a fundamental domain must be redefined.

The projections $\Lambda_\parallel$ of the lattice basis vectors of P or D_6 to $E_\parallel$ provide two of the three irreducible icosahedral modules [14] in the form $\Lambda_\parallel$.

For the scaling symmetry [14] we use the projectors $P_\parallel = M^{-1}I_\parallel M$, $P_\perp = M^{-1}I_\perp M$ to the subspaces $E_\parallel$, $E_\perp$. We define with $\tau := (1+\sqrt{5})/2$ the matrix

$$S(\tau) = \tau P_\parallel - (1/\tau)P_\perp = (1/2)\begin{bmatrix} 1 & 1 & 1 & \bar{1} & \bar{1} & 1 \\ 1 & 1 & 1 & \bar{1} & \bar{1} & \bar{1} \\ 1 & 1 & 1 & 1 & \bar{1} & \bar{1} \\ 1 & \bar{1} & 1 & 1 & 1 & \bar{1} \\ 1 & \bar{1} & \bar{1} & 1 & 1 & 1 \\ 1 & 1 & \bar{1} & \bar{1} & 1 & 1 \end{bmatrix}. \tag{11}$$

The scaling symmetries of the lattices can now be expressed in the basis of P as

$$(S(\tau))^3 = S(\tau^3): \ P \to P \qquad S(\tau): \ D_6 \to D_6 \tag{12}$$

where the matrix S is to be applied from the right to the basis vectors equation (5).

8. The icosahedral tilings $(\mathcal{T}^*, P/D_6)$

The tiling $(\mathcal{T}^*, P)$ [14] belongs to the primitive hypercubic lattice $\Lambda = P \subset E^6$ equation (4). Both the Voronoi and Delone cells are unit hypercubes with centres at lattice points $q = (000000) + P$ and hole points $h = (1111111)/2 + P$ respectively. The projection $\Lambda_\parallel$ is the primitive icosahedral module. Its module basis is the six vectors $(e_{1\parallel}, \ldots, e_{6\parallel})$ given by the entries of the first three rows of the matrix M in equation (9). In $E_\parallel$, $E_\perp$ they point along fivefold axes. The tiles are an obtuse and an oblate rhombohedron, which we denote by $(F^*, G^*)_\parallel$. The vertex window, the projected hypercube $V_\perp$, is Kepler's triacontahedron. The dual windows for the tiles are rhombohedra $(F, G)_\perp$.

The tiling $(\mathcal{T}^*, D_6)$ [12] belongs to the face-centred hypercubic lattice with the basis equation (5). There are three Delone cells D^a, D^b, D^c located at three types of hole $h = a, b, c$. Their representatives are given in table 1. The projection $\Lambda_\parallel = (D_6)_\parallel$ is the icosahedral $2F$-module. Its module basis is the six vectors $(b_{1\parallel}, \ldots, b_{6\parallel})$ from equation (5). In $E_\parallel$ they point along twofold axes. The tiles are six tetrahedra $(A^*, B^*, C^*, D^*, F^*, G^*)_\parallel$. The Voronoi cell V for $\Lambda = D_6$ differs from the hypercube, but its projection $V_\perp$, the vertex window of the tiling, is again a triacontahedron. The dual windows $(A, B, C, D, F, G)_\perp$ are four pyramids with a standard rhombus base and two rhombohedra which in shape coincide with the ones of the primitive tiling. The tiling $(\mathcal{T}^*, P)$ is obtained from $(\mathcal{T}^*, D_6)$ by blowing up the tetrahedral tiles $(F^*, G^*)_\parallel$ into rhombohedra and omitting all other tiles. Tiles and windows in detail are given in tables 4–6.

Table 1. Representative hole positions in the window $V_\perp$.

Type	Position h_i	Distance	|Orbit|
c	$\frac{1}{2}(11\overline{1}\overline{1}1\overline{1})$	τ⑤	12
	$\frac{1}{2}(\overline{1}11\overline{1}1\overline{1})$	③	20
a	$\frac{1}{2}(111\overline{1}1\overline{1})$	τ③	20
	$\frac{1}{2}(11\overline{1}\overline{1}11)$	τ^{-1}⑤	12
b	(000001)	⑤	12

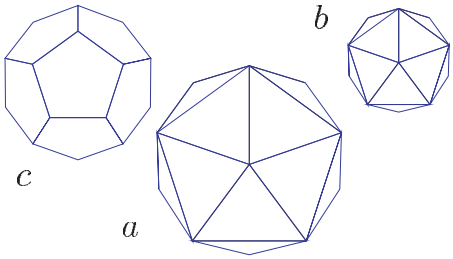

Figure 2. Delone clusters for $\Lambda = D_6$: $D^a_\parallel$, $D^b_\parallel$ are icosahedra (edge length τ②, ②), $D^c_\parallel$ is a dodecahedron (edge length ②). For $\Lambda = P$ the Delone clusters are Kepler's triacontahedra $V_\parallel$ (edge length ②).

(This figure is in colour only in the electronic version, see `www.iop.org`)

9. Delone clusters in the icosahedral tilings ($\mathcal{T}^*$, P/D_6)

In the primitive hypercubic lattice $\Lambda = P$ both the Voronoi and the single Delone cell are hypercubes. Under icosahedral projection they become Kepler's triacontahedra. There are three types of hole and Delone cells D^a, D^b, D^c in $\Lambda = D_6$. The Delone clusters $D^h_\parallel$ are shown in figure 2. The hole positions are given in table 1. ⑤, ② and ③ denote standards of length [12] along 5-, 2- and 3-axes,

$$⑤ = \sqrt{\frac{1}{2}} \qquad ② = \sqrt{\frac{2}{\tau+2}} \qquad ③ = \sqrt{\frac{3}{2\tau+2}}. \tag{13}$$

We summarize here the results of the analysis given in sections 10–13.

Proposition 14 (Delone clusters in ($\mathcal{T}^*$, P/D_6)).

(1) The windows $w(D^h_\parallel)$ for fixed orientation are parts of Coxeter cones with closest axis sets $(\tau^{-1})(②/2, ⑤/\tau, ③/\tau)$, bounded by a plane through the endpoints of these axes.

(2) The G-windows under H_3 applied with respect to the hole position $h_\parallel$ are scaled triacontahedra $w_{H_3}(D^{(a,c)}_\parallel) = w_{H_3}(V_\parallel) = \tau^{-2}V_\perp$, $w_{H_3}(D^b_\parallel) = \tau^{-3}V_\perp$ centred at representative hole positions $h_\perp$ of table 1. If $h_\perp$ is a point on the boundary of $V_\perp$, the scaled triacontahedron centred at $h_\perp$ reduces to its intersection with $V_\perp$.

(3) The Delone clusters for fixed orientation are uniquely filled by tiles, as summarized in tables 2 and 3 and given in detail in tables 4–6. The filling breaks the local icosahedral symmetry. No orientation of any tile is repeated within the filling. The filling of the Delone clusters in $(\mathcal{T}^*, P)$ arises from that of $D^{(a,c)}_\parallel$ in $(\mathcal{T}^*, D_6)$ by blowing up $(F^*, G^*)_\parallel$ into rhombohedra and omitting all other tiles.

(4) The Delone clusters $D^a_\parallel$, $D^b_\parallel$, $D^c_\parallel$ and their mirror images together do not form a fundamental domain $\mathcal{F}(\mathcal{T}^*, D_6)$, table 2. Kepler's [8] triacontahedron $V_\parallel = \mathcal{F}(\mathcal{T}^*, P)$ is a fundamental domain, table 3.

Table 2. Number of tiles in Delone clusters and in $\mathcal{F} = \mathcal{F}(\mathcal{T}^*, D_6)$, see table 8.

Tile	$A_\parallel^*$	$B_\parallel^*$	$C_\parallel^*$	$D_\parallel^*$	$F_\parallel^*$	$G_\parallel^*$	
$D_\parallel^a$	3	1	16		8	10	10
$D_\parallel^b$	1	7	2		6	—	—
$D_\parallel^c$	7	3	4		4	10	10
$\mathcal{F}$	30	30	60		60	20	20

Table 3. Number of tiles in Delone clusters $V_\parallel$ and in $\mathcal{F} = \mathcal{F}(\mathcal{T}^*, P)$.

Tile	$F_\parallel$	$G_\parallel$
$V_\parallel, \mathcal{F}$	10	10

(5) The Delone G-windows cover $V_\perp$ up to a fraction τ^{-9}. This means that 98.7 per cent of the vertices in the tiling are covered by Delone clusters.

Kepler's triacontahedron [8], the icosahedral projection of the six-dimensional hypercube, appeared as a window at the beginning of quasicrystallography. Now it arises as a Delone cluster in icosahedral quasicrystals.

10. Filling of icosahedral Delone clusters

From proposition 11 we must construct in $E_\perp$ at each hole position $h = a, c, b$ a maximal intersection of coding tiles. All solid angles at hole positions of the coding tiles contain an equal number of right and left spherical Coxeter cones of volume $\omega = 4\pi/120$, each one spanned by a closest set of two-, five- and threefold axes. The Coxeter cone must be redefined in $E_\perp$ in line with the representation $\mathcal{D}_\perp(H_3)$. It is easy to see that the intersection of coding tiles in all three cases will be part of a Coxeter cone in $E_\perp$ bounded by plane(s). We shall choose in $E_\perp$ an initial infinite Coxeter cone defined by the three vectors

$$\begin{aligned}
&(e_1 + e_5)_\perp/2 \qquad |(e_1 + e_5)_\perp|/2 = ②/2\\
&(+e_1 + e_2 - e_3 - e_4 + e_5 + e_6)_\perp/2 \qquad |(+e_1 + e_2 - e_3 - e_4 + e_5 + e_6)_\perp|/2 = ⑤/\tau \qquad (14)\\
&(e_1 + e_2 + e_3)_\perp \qquad |(e_1 + e_2 + e_3)_\perp| = ③/\tau
\end{aligned}$$

which form a closest set of two-, five- and threefold axes. This amounts to fixing a single orientation for the coding and filling. The coding tiles in $E_\perp$ are denoted by X, the tiles in the filling by their duals X^*. The relation between the two is taken from [14]. In tables 4–6 we give a complete algebraic description of all the tiles and windows in standard positions. In [14] the expressions for the boundaries refer to a lattice point q and so we write them as $X(q)$, $X^*(q)$. To apply proposition 11 we must rewrite the boundaries as $X(h)$, $X^*(h)$ where the boundary $X(h)$ is seen from one of its specific vertex and hole points h. The two expressions are related by a shift

$$X(h) = X(q) + t \qquad t = h - q \qquad X^*(h) = X^*(q) + t. \qquad (15)$$

Consider a standard fixed pair of dual boundaries $X(h)$, $X^*(h)$. All other copies of $X(h)$ which contribute to the intersection $\bigcap_j X_{j\perp}(h)$ of proposition 11 are obtained by the action of icosahedral rotations $g : X(h) \to gX(h)$. The rotation g refers to the hole point h and can be expressed as a permutation of the basis vectors $(e_1, \ldots, e_6)$ in E^6. Permutations are given in signed cycle notation. The coding and the filling boundaries in proposition 11 can then be listed as follows:

(i) Choose an initial Coxeter cone in $E_\perp$ at a hole position $h = a, c$ or b.

(ii) For $X_\perp(h) = (A, B, C, D, F, G)_\perp(h)$ choose a standard position of $X_\perp(h)$ which contains interior points of the initial Coxeter cone. If the boundary $X_\perp$ has several hole positions of the same type h not connected by a local symmetry of the boundary, each one must be treated separately. We distinguish these hole positions by Greek indices $\alpha, \beta, \ldots$.

(iii) For one such choice, the boundary $X_\perp(h)$ in standard position at $h_\perp$ spans a solid angle Ω which in all cases is composed from an equal number of (right and left) spherical Coxeter cones each of solid angle $\omega = 4\pi/120$. By ν we denote the number of rotated occurrences of a tile window. This number is obtained from the total solid angle Ω at the hole vertex $h_\perp$ as $\nu = \Omega/(2\omega)$. The division by the factor 2 arises because we only count right Coxeter cones within Ω. An exception in this counting arises for the cases when $X_{j\perp}$ as a polytope has a rotational symmetry with respect to the hole position $h_\perp$. Such rotational symmetries occur at $F(a)(\beta)$, $G(a)(\beta)$, $F(c)(\beta)$, $G(c)(\beta)$, $A(b)$, $B(b)$ (see tables 4–6). For any right Coxeter cone contained in Ω there is an icosahedral rotation g which maps it into the initial Coxeter cone. It follows that $gX_\perp(h)$ contributes to the intersection. The set of these rotations we denote by $S(X)$, $|S(X)| = \nu$. The complete window equation (2) can now be written as

$$w(D^h_\parallel) = \bigcap_j X_{j\perp}(h) = \bigcap \Bigg(\Bigg(\bigcap_{g\in S(A)} gA_\perp(h) \Bigg) \times \Bigg(\bigcap_{g\in S(B)} gB_\perp(h) \Bigg) \cdots \Bigg(\bigcap_{g\in S(G)} gG_\perp(h) \Bigg) \Bigg). \tag{16}$$

(iv) After constructing in this fashion a complete list of coding tiles in the intersection, we look for the tiles which by their faces bound the initial Coxeter cone. The result is that the bound is always given by a single plane perpendicular to the twofold axis. The bounded Coxeter cone then belongs to a triacontahedron around $h_\perp$ which for $h = a, c$ is $\tau^{-2}V_\perp$ and for $h = b$ is $\tau^{-3}V_\perp$.

(v) The positions of $X^*_\parallel(h)$ which contribute to the filling are by proposition 11 in one-to-one correspondence to $S(X)$. We list in the same order the dual boundaries $X^*(h) = (A^*, B^*, C^*, D^*, F^*, G^*)(h)$. The filling of the Delone cell D^h at fixed orientation is given by rewriting equation (3) in detail as

$$D^h_\parallel = \bigcup_j X^*_{j\parallel}(h) = \bigcup \Bigg(\Bigg(\bigcup_{g\in S(A)} gA^*_\parallel(h) \Bigg) \Bigg(\bigcup_{g\in S(B)} gB^*_\parallel(h) \Bigg) \cdots \Bigg(\bigcup_{g\in S(G)} gG^*_\parallel(h) \Bigg) \Bigg). \tag{17}$$

In tables 4–6, we use the following rules in $E_\perp$ for the inflation of vectors along three- and fivefold axes derived from equation (11):

$i_3 =$ ((narrow forward triple) − (wide forward triple))/2,
$\tau i_3 =$ ((narrow forward triple) + (wide forward triple))/2,
$\tau i_5 = \tau e_{i\perp} =$ (forward quintuple + $e_{i\perp}$)/2
$\tau^{-1} i_5 = e_{i\perp}/\tau =$ (forward quintuple − $e_{i\perp}$)/2.

Tables 4–6. For each pair of dual boundaries $X(h)$, $X^*(h)$ we list the standard positions, the numbers ν and Ω defined under (iii) and (iv) and the set $S(X)$ of orientations, given as signed permutations g applied to the standard position, which contribute to the intersection and filling. Coefficients in front of vectors always range as $0 \leqslant \mu_j \leqslant 1$. The brackets $\langle , \rangle$ denote the convex hull of the vectors included. A circle $\circ$ denotes the join of two polytopes. The

Table 4. Delone cluster D^a.

$A(a) = (-\mu_4 e_4 - \mu_6 e_6) \circ (-e_1 + e_2 + e_3 - e_4 + e_5 - e_6)/2$
$A^*(a) = \langle -e_2, -e_3, -e_5, e_1\rangle + (-e_1 + e_2 + e_3 - e_4 + e_5 - e_6)/2$
$\nu = 3, \Omega = 6\omega$
$S(A):\quad e \quad (132)(4\bar{5}\bar{6}) \quad (123)(46\bar{5})$

$B(a) = (-\mu_4 e_4 - \mu_6 e_6) \circ (-e_1 - e_2 - e_3 - e_4 + e_5 - e_6)/2$
$B^*(a) = \langle e_2, e_3, -e_5, e_1\rangle + (-e_1 - e_2 - e_3 - e_4 + e_5 - e_6)/2$
$\nu = 1, \Omega = 2\omega$
$S(B):\quad e$

$C(a)(\alpha) = (\mu_1 e_1 + \mu_5 e_5) \circ (e_1 + e_2 - e_3 - e_4 + e_5 - e_6)/2$
$C^*(a)(\alpha) = \langle -e_2, e_3, e_4, e_6\rangle + (e_1 + e_2 - e_3 - e_4 + e_5 - e_6)/2$
$\nu = 3, \Omega = 6\omega$
$S(C,\alpha):\quad e \quad (1\bar{4}52\bar{3}) \quad (132)(4\bar{5}\bar{6})$

$C(a)(\beta) = (\mu_1 e_1 + \mu_5 e_5) \circ (e_1 + e_2 - e_3 + e_4 + e_5 + e_6)/2$
$C^*(a)(\beta) = \langle -e_2, e_3, -e_4, -e_6\rangle + (e_1 + e_2 - e_3 + e_4 + e_5 + e_6)/2$
$\nu = 13, \Omega = 26\omega$
$S(C,\beta):\quad e \quad (12\bar{4}3\bar{5}) \quad (1\bar{4}52\bar{3}) \quad (1\bar{3}25\bar{4})$
$(15\bar{3}4\bar{2}) \quad (132)(4\bar{5}\bar{6}) \quad (2\bar{4})(5\bar{6})(1\bar{1})(3\bar{3}) \quad (1\bar{2}64\bar{3}) \quad (134)(2\bar{6}5)$
$(1\bar{6}\bar{4})(23\bar{5}) \quad (25364) \quad (1\bar{4}36\bar{5}) \quad (1\bar{3}\bar{6})(2\bar{4}\bar{5})$

$D(a)(\alpha) = (\mu_1 e_1 + \mu_5 e_5) \circ (e_1 + e_2 + e_3 + e_4 + e_5 - e_6)/2$
$D^*(a)(\alpha) = \langle -e_2, -e_3, -e_4, e_6\rangle + (e_1 + e_2 + e_3 + e_4 + e_5 - e_6)/2$
$\nu = 4, \Omega = 8\omega$
$S(D,\alpha):\quad e \quad (1\bar{4}52\bar{3}) \quad (1\bar{3}25\bar{4}) \quad (132)(4\bar{5}\bar{6})$

$D(a)(\beta) = (\mu_1 e_1 + \mu_5 e_5) \circ (e_1 - e_2 - e_3 + e_4 + e_5 - e_6)/2$
$D^*(a)(\beta) = \langle e_2, e_3, -e_4, e_6\rangle + (e_1 - e_2 - e_3 + e_4 + e_5 - e_6)/2$
$\nu = 4, \Omega = 8\omega$
$S(D,\beta):\quad e \quad (1\bar{4}52\bar{3}) \quad (132)(4\bar{5}\bar{6}) \quad (1\bar{6}\bar{4})(23\bar{5})$

$F(a)(\alpha) = (-\mu_4 e_4 - \mu_6 e_6 - \mu_1 e_1)$
$F^*(a)(\alpha) = \langle 0, -e_2 - e_3, -e_3 + e_5, e_5 - e_2\rangle + (-e_1 + e_2 + e_3 - e_4 - e_5 - e_6)/2$
$\nu = 9, \Omega = 18\omega$
$S(F,\alpha):\quad e \quad (1\bar{3}25\bar{4}) \quad (132)(4\bar{5}\bar{6}) \quad (2\bar{4})(5\bar{6})(1\bar{1})(3\bar{3})$
$(143)(25\bar{6}) \quad (123)(46\bar{5}) \quad (1\bar{2}35\bar{6}) \quad (1\bar{5}63\bar{4}) \quad (162)(35\bar{4})$

$F(a)(\beta) = (-\mu_4 e_4 - \mu_6 e_6 + \mu_5 e_5)$
$F^*(a)(\beta) = \langle 0, -e_2 - e_3, -e_3 - e_1, -e_1 - e_2\rangle + (e_1 + e_2 + e_3 - e_4 + e_5 - e_6)/2$
$\nu = 1, \Omega = 6\omega$
$S(F,\beta):\quad e$

$G(a)(\alpha) = (\mu_1 e_1 + \mu_5 e_5 - \mu_6 e_6)$
$G^*(a)(\alpha) = \langle 0, -e_2 + e_3, e_3 - e_4, -e_4 - e_2\rangle + (e_1 + e_2 - e_3 + e_4 + e_5 - e_6)/2$
$\nu = 3, \Omega = 6\omega$
$S(G,\alpha):\quad e \quad (1\bar{4}52\bar{3}) \quad (132)(4\bar{5}\bar{6})$

$G(a)(\beta) = (\mu_1 e_1 + \mu_5 e_5 + \mu_4 e_4)$
$G^*(a)(\beta) = \langle 0, -e_2 + e_3, e_3 + e_6, e_6 - e_2\rangle + (e_1 + e_2 - e_3 + e_4 + e_5 - e_6)/2$
$\nu = 7, \Omega = 42\omega$
$S(G,\beta):\quad e \quad (12\bar{4}3\bar{5}) \quad (1\bar{4}52\bar{3}) \quad (1\bar{3}25\bar{4})$
$(15\bar{3}4\bar{2}) \quad (132)(4\bar{5}\bar{6}) \quad (1\bar{6}\bar{4})(23\bar{5})$

boundaries $X = A, B, C, D$ are joins of a rhombus and a point outside the rhombus plane. The symbols $_{\parallel,\perp}$ are omitted since there is a unique lifting. The windows and fillings are formed upon projecting the shifts and boundaries X, X^* to $E_\perp$ and $E_\parallel$ respectively. All these filling constructions are made with one single Coxeter cone, hence with a single orientation.

Table 5. Delone cluster D^c.

$A(c) = (\mu_1 e_1 + \mu_5 e_5) \circ (e_1 + e_2 - e_3 + e_4 + e_5 - e_6)/2$
$A^*(c) = \langle -e_2, e_3, -e_4, e_6\rangle + (e_1 + e_2 - e_3 + e_4 + e_5 - e_6)/2$
$\nu = 7, \Omega = 14\omega$
$S(A):$ e $(12\bar{4}\bar{3}5)$ $(1\bar{4}52\bar{3})$ $(1\bar{3}25\bar{4})$
$(15\bar{3}\bar{4}2)$ $(132)(4\bar{5}6)$ $(1\bar{6}\bar{4})(23\bar{5})$

$B(c) = (\mu_1 e_1 + \mu_5 e_5) \circ (e_1 + e_2 - e_3 - e_4 + e_5 + e_6)/2$
$B^*(c) = \langle -e_2, e_3, e_4, -e_6\rangle + (e_1 + e_2 - e_3 - e_4 + e_5 + e_6)/2$
$\nu = 3, \Omega = 6\omega$
$S(B):$ e $(1\bar{4}52\bar{3})$ $(132)(4\bar{5}6)$

$C(c)(\alpha) = (-\mu_4 e_4 - \mu_6 e_6) \circ (-e_1 + e_2 - e_3 - e_4 + e_5 - e_6)/2$
$C^*(c)(\alpha) = \langle -e_2, e_3, e_1, -e_5\rangle + (-e_1 + e_2 - e_3 - e_4 + e_5 - e_6)/2$
$\nu = 2, \Omega = 4\omega$
$S(C, \alpha):$ e $(1\bar{3}25\bar{4})$

$C(c)(\beta) = (-\mu_4 e_4 - \mu_6 e_6) \circ (-e_1 - e_2 + e_3 - e_4 + e_5 - e_6)/2$
$C^*(c)(\beta) = \langle 2, -3, 1, -5\rangle + (-e_1 - e_2 + e_3 - e_4 + e_5 - e_6)/2$
$\nu = 2, \Omega = 4\omega$
$S(C, \beta):$ e $(123)(46\bar{5})$

$D(c)(\alpha) = (-\mu_4 e_4 - \mu_6 e_6) \circ (e_1 + e_2 + e_3 - e_4 + e_5 - e_6)/2$
$D^*(b)(\alpha) = \langle -e_2, -e_3, -e_1, -e_5\rangle + (e_1 + e_2 + e_3 - e_4 + e_5 - e_6)/2$
$\nu = 1, \Omega = 2\omega$
$S(D, \alpha):$ e

$D(c)(\beta) = (-\mu_4 e_4 - \mu_6 e_6) \circ (-e_1 + e_2 + e_3 - e_4 - e_5 - e_6)/2$
$D^*(c)(\beta) = \langle -2, -3, 1, 5\rangle + (-e_1 + e_2 + e_3 - e_4 - e_5 - e_6)/2$
$\nu = 3, \Omega = 6\omega$
$S(D, \beta):$ e $(123)(46\bar{5})$ $(132)(4\bar{5}6)$

$F(c)(\alpha) = (-\mu_4 e_4 - \mu_6 e_6 - \mu_1 e_1) + (-e_1 - e_2 - e_3 - e_4 + e_5 - e_6)/2$
$F^*(c)(\alpha) = \langle 0, e_2 + e_3, e_2 - e_5, e_3 - e_5\rangle + (-e_1 - e_2 - e_3 - e_4 + e_5 - e_6)/2$
$\nu = 9, \Omega = 18\omega$
$S(F, \alpha):$ e $(1\bar{3}25\bar{4})$ $(132)(4\bar{5}6)$ $(2\bar{4})(5\bar{6})(1\bar{1})(3\bar{3})$
$(143)(25\bar{6})$ $(123)(46\bar{5})$ $(1\bar{2}35\bar{6})$ $(1\bar{5}63\bar{4})$ $(162)(35\bar{4})$

$F(c)(\beta) = (-\mu_4 e_4 - \mu_6 e_6 + \mu_5 e_5) + (-e_1 - e_2 - e_3 - e_4 + e_5 - e_6)/2$
$F^*(c)(\beta) = \langle 0, e_2 + e_3, e_3 + e_1, e_1 + e_2\rangle + (-e_1 - e_2 - e_3 - e_4 + e_5 - e_6)/2$
$\nu = 1, \Omega = 6\omega$
$S(F, \beta):$ e

$G(c)(\alpha) = (\mu_1 e_1 + \mu_5 e_5 - \mu_6 e_6) + (e_1 - e_2 + e_3 - e_4 + e_5 - e_6)/2$
$G^*(c)(\alpha) = \langle 0, e_2 - e_3, -e_3 + e_4, e_4 + e_2\rangle + (e_1 - e_2 + e_3 - e_4 + e_5 - e_6)/2$
$\nu = 3, \Omega = 6\omega$
$S(G, \alpha):$ e $(1\bar{4}52\bar{3})$ $(132)(4\bar{5}6)$

$G(c)(\beta) = (\mu_1 e_1 + \mu_5 e_5 + \mu_4 e_4)$
$G^*(c)(\beta) = \langle 0, e_2 - e_3, -e_3 - e_6, -e_6 + e_2\rangle + (e_1 - e_2 + e_3 + e_4 + e_5 + e_6)/2$
$\nu = 7, \Omega = 42\omega$
$S(G, \beta):$ e $(12\bar{4}\bar{3}5)$ $(1\bar{4}52\bar{3})$ $(1\bar{3}25\bar{4})$
$(15\bar{3}\bar{4}2)$ $(132)(4\bar{5}6)$ $(1\bar{6}\bar{4})(23\bar{5})$

The filling construction given in tables 4–6 was based on a single Coxeter cone. By application of the reflection $R_1 = (23)(46)$ equation (8) with respect to the chosen hole point h we obtain a mirror image of this Coxeter cone which gives rise to a mirror filling. To obtain this mirror filling, we apply this reflection to the expressions of equations (16) and (17). Then all the operations (translations and permutations) in tables 4–6 must be replaced by

Table 6. Delone cluster D^b.

$A(b) = (-\mu_2 e_2 + \mu_3 e_3 + (e_1 + e_2 - e_3 - e_4 + e_5 - e_6)/2) \circ 0$
$A^*(b) = \langle e_1, -e_6, e_5, -e_4 \rangle$
$\nu = 1, \Omega = 4\omega$
$S(A):\quad e$

$B(b) = (-\mu_2 e_2 + \mu_3 e_3 + (-e_1 + e_2 - e_3 - e_4 - e_5 - e_6)/2) \circ 0$
$B^*(b) = \langle -e_5, -e_4, -e_1, -e_6 \rangle$
$\nu = 7, \Omega = 28\omega$
$S(B):\quad e \quad (12\bar{4}\bar{3}5) \quad (1\bar{3}25\bar{4}) \quad (123)(46\bar{5})$
$(1\bar{3}46\bar{2}) \quad (132)(4\bar{5}6) \quad (1\bar{2}35\bar{6})$

$C(b) = (\mu_5 e_5 - \mu_3 e_3 + (e_1 + e_2 + e_3 - e_4 - e_5 - e_6)/2) \circ 0$
$C^*(b) = \langle e_1, -e_6, e_2, -e_4 \rangle$
$\nu = 2, \Omega = 4\omega$
$S(C):\quad e \quad (1\bar{4}52\bar{3})$

$D(b) = (\mu_2 e_2 + \mu_3 e_3 + (e_1 - e_2 - e_3 + e_4 + e_5 - e_6)/2) \circ 0$
$D^*(b) = \langle e_1, -e_6, e_4, e_5 \rangle$
$\nu = 6, \Omega = 12\omega$
$S(D):\quad e \quad (12\bar{4}\bar{3}5) \quad (1\bar{4}52\bar{3}) \quad (1\bar{3}25\bar{4})$
$(15\bar{3}\bar{4}2) \quad (15)(46)(2\bar{2})(3\bar{3})$

Table 7. Volume composition $|X_j^*|$, $|X_j|$ as a fraction of V_0.

$X_\parallel^*$	A^*	B^*	C^*	D^*	F^*	G^*
$\lvert X^*\rvert/V_0$	$2\tau+1$	1	$\tau+1$	τ	$\tau+1$	τ
$X_\perp$	A	B	C	D	F	G
$\lvert X\rvert/V_0$	$2\tau+1$	1	$\tau+1$	τ	$3\tau+3$	3τ
μ	30	30	60	60	20	20

their conjugates with respect to (23)(46), and the windows and tiles in standard position are transformed as $X \to (23)(46)X$, $X^* \to (23)(46)X^*$.

The mirror windows in the transformed equation (16) have the same outer shape but a reflected standard position. The mirror windows contribute to the G-windows and convert them into the full scaled triacontahedra given in proposition 14. The transformed equation (17) determines a new mirror filling of the Delone clusters $D_\parallel^a$, $D_\parallel^c$ but transforms the filling of $D_\parallel^b$ into itself.

11. Volume composition of Delone clusters in $(\mathcal{T}^*, D_6)$.

The filling and fundamental domain properties for the tilings imply sum rules in terms of the volumes of the tiles. They are given in this section.

In table 7 we give the volumes for the pairs of tiles of the tiling $(\mathcal{T}^*, D_6)$. In the last row we list the number μ of translational orbits for the 3-boundaries whose projections are the tiles and their duals. We define

$$V_0 := \frac{1}{12}\left[\frac{2}{\tau+2}\right]^{3/2} = \frac{\tau^{-2}}{15}\sqrt{\frac{\tau+2}{2}}. \tag{18}$$

In tables 8–10 we give for the three Delone cells the volume composition in terms of the tiles X_j^*. For each tile and its hole vertex type $\alpha, \beta \ldots$ we repeat from tables 4–6 the solid angle $\Omega = 2\nu\omega$ as a multiple of the solid angle $\omega = 4\pi/120$ for the fundamental spherical

Table 8. Volume composition of Delone cluster $D^a_\parallel$.

X^*_j	$2\nu := \Omega/\omega$	C_m	(ν/m)	$\sum(\nu/m)$	$\lvert X^*_j\rvert/V_0$	$(\nu/m)\lvert X^*_j\rvert/V_0$
A^*	6	C_1	3	3	$2\tau+1$	$6\tau+3$
B^*	2	C_1	1	1	1	1
C^*,α	6	C_1	3		$\tau+1$	$3\tau+3$
C^*,β	26	C_1	13	16	$\tau+1$	$13\tau+13$
D^*,α	8	C_1	4		τ	4τ
D^*,β	26	C_1	4	8	τ	4τ
F^*,α	18	C_1	9		$\tau+1$	$9\tau+9$
F^*,β	6	C_3	1	10	$\tau+1$	$\tau+1$
G^*,α	6	C_1	3		τ	3τ
G^*,β	42	C_3	7	10	τ	7τ
$D^a_\parallel$						$50\tau+30$

Table 9. Volume composition of Delone cluster $D^c_\parallel$.

X^*_j	$2\nu := \Omega/\omega$	C_m	(ν/m)	$\sum(\nu/m)$	$\lvert X^*_j\rvert/V_0$	$(\nu/m)\lvert X^*_j\rvert/V_0$
A^*	14	C_1	7	7	$2\tau+1$	$14\tau+7$
B^*	6	C_1	3	3	1	3
C^*,α	4	C_1	2		$\tau+1$	$2\tau+2$
C^*,β	4	C_1	2	4	$\tau+1$	$2\tau+2$
D^*,α	2	C_1	1		τ	τ
D^*,β	6	C_1	3	4	τ	3τ
F^*,α	18	C_1	9		$\tau+1$	$9\tau+9$
F^*,β	6	C_3	1	10	$\tau+1$	$\tau+1$
G^*,α	6	C_1	3		τ	3τ
G^*,β	42	C_3	7	10	τ	7τ
$D^c_\parallel$						$42\tau+24$

Table 10. Volume composition of Delone cluster $D^b_\parallel$.

X^*_j	$2\nu := \Omega/\omega$	C_m	(ν/m)	$\sum(\nu/m)$	$\lvert X^*_j\rvert/V_0$	$(\nu/m)\lvert X^*_j\rvert/V_0$
A^*	4	C_2	1	1	$2\tau+1$	$2\tau+1$
B^*	28	C_2	7	7	1	7
C^*	4	C_1	2	2	$\tau+1$	$2\tau+2$
D^*	12	C_1	6	6	τ	6τ
$D^b_\parallel$						$10\tau+10$

Coxeter cone and the rotational point group C_m that preserves the vertex and the tile. Next we give the number ν/m of occurrences of the tile X^*_j in the Delone cell, first separate for each vertex type α, β and then summed, and its volume $|X^*_j|/V_0$, where V_0 is given in equation (18). Finally we list the relative volume contribution $(\nu/m)|X^*_j|/V_0$. The sum of the entries of the last column yields the volume $|D^h|/V_0$.

12. Fundamental domains and icosahedral tilings

We apply the notions on fundamental domains as defined in section 5 definitions 6–8 to the lattices Λ and icosahedral tilings $(\mathcal{T}^*, \Lambda)$. There are basic sets of six-dimensional klotz cells which together form a fundamental domain according to definitions 6 and 7 for the

six-dimensional lattices. The volume of a six-dimensional klotz cell from equation (1) is the product of the three-dimensional volumes of projected dual boundaries given in table 7. We check the sum rule that connects the volumes of the klotz cells with the volume of the six-dimensional fundamental domain of the lattice according to proposition 3.

Tiling $(\mathcal{T}, P)$. Rhombohedral tiles of shape and volume F, G each in ten orientations. The sum over products

$$V(\mathcal{T}, P) = 10|F_\perp||F_\parallel^*| + 10|G_\perp||G_\parallel^*| = 10[(3\tau)^2 + (3\tau^2)^2]V_0^2 = 1 \tag{19}$$

is equal to the volume of the six-dimensional unit hypercube.

Next we explore the fundamental domain properties according to definitions 8 and 9. From the two projected tiles each with ten orientations we obtain for the tiling *fundamental domains* of size

$$|\mathcal{F}(\mathcal{T}, P)| = 10(|F_\parallel| + |G_\parallel|) \tag{20}$$

$$= 10(3\tau + 3\tau^2)V_0 = 30\tau^3 V_0 = |V_\parallel| \tag{21}$$

equal to the volume of the projected Voronoi cluster $V_\parallel$. The window of the tiling is $V_\perp$. This is consistent with

Proposition 15. *The triacontahedral Delone clusters $V_\parallel$ of the tiling $(\mathcal{T}, P)$ each form a fundamental domain comprising* 10 *obtuse and* 10 *oblate rhombohedra.*

Tiling $(\mathcal{T}^*, D_6)$. The sum over products

$$\begin{aligned} V(\mathcal{T}^*, D_6) &= 30(|A_\parallel^*||A_\perp| + |B_\parallel^*||B_\perp|) + 60(|C_\parallel^*||C_\perp| + |D_\parallel^*||D_\perp|) \\ &\quad +20(|F_\parallel^*||F_\perp| + |G_\parallel^*||G_\perp|) \\ &= [30((\tau^6 + 1^2) + 60(\tau^4 + \tau^2) + 20(3\tau^4 + 3\tau^2)]V_0^2 = 2 \end{aligned} \tag{22}$$

is equal to the volume of the six-dimensional Voronoi cell of D_6 given as $\sqrt{\det} = 2$ in [3, p 117]. The fundamental domain for the tiling $(\mathcal{T}^*, D_6)$ according to definitions 8 and 9 has the size

$$\begin{aligned} |\mathcal{F}(\mathcal{T}^*, D_6)| &= 30(|A_\parallel^*| + |B_\parallel^*|) + 60(|C_\parallel^*| + |D_\parallel^*|) + 20(|F_\parallel^*| + |G_\parallel^*|) \\ &= [30(2\tau + 2) + 60(2\tau + 1) + 20(2\tau + 1)]V_0 \\ &= 20\tau^4(\tau + 2)V_0. \end{aligned} \tag{23}$$

From the orientations of the tiles in the fillings given in tables 4–6 it can be verified that the three filled Delone clusters if combined do not form a fundamental domain for the tiling. This can also be seen from the volumes: if the fillings of the Delone clusters together would form a fundamental domain according to definitions 8 and 9, the volumes of the three Delone cells given in tables 8–10 should add up to the value given in equation (23), which is not the case.

13. Covering by icosahedral Delone clusters

We consider here the covering of vertex points in the icosahedral tilings by Delone clusters and use proposition 12.

Tiling $(\mathcal{T}^*, P)$. To examine the covering of this icosahedral tiling by the Delone clusters $V_\parallel$ it suffices to check the intersection $Co_\perp$ of one Coxeter cone with the triacontahedral window $V_\perp$. Its radial edges are closest axis sets $((\tau^2/2)\textcircled{2}, \tau\textcircled{5}, \tau\textcircled{3})$, scaled by τ^2 compared with equation (13). Its volume is $|Co_\perp| = |V_\perp|/120 = (\tau^3/4)V_0$. The G-windows are

triacontahedra $\tau^{-2}V_\perp$ located at the hole positions of type (a, c) given in table 1 and intersected with $V_\perp$. Inspection of the position of these windows within the cone $Co_\perp$ yields:

All points of $Co_\perp$ are covered except for a convex polytope $H_\perp$ located in the simpleton vertex window. The volume of this uncovered window polytope can be expressed in terms of V_0 as

$$|H_\perp| = (\tau^{-6}/4)V_0. \tag{24}$$

Comparing with the Coxeter cone we obtain

$$|H_\perp|/|Co_\perp| = (\tau^{-6}/4)(4/\tau^3) = \tau^{-9}. \tag{25}$$

which is 1.3 per cent. From this result we obtain

Proposition 16. *The Delone clusters $V_\parallel$ cover 98.7 per cent of the vertices in the tiling $(\mathcal{T}^*, P)$.*

Tiling $(\mathcal{T}^*, D_6)$. Here the Delone clusters are different, but their windows are the same as before. A similar analysis of the same Coxeter cone $Co_\perp$ shows:

(i) The Coxeter cone is already covered by the G-windows for the holes of type (a, c). Therefore any vertex point of the tiling covered by a Delone cluster $D^b_\parallel$ is already covered by a cluster $D^a_\parallel$ or $D^c_\parallel$.

(ii) The uncovered window polytope coincides with $H_\perp$. Therefore the percentage of the covering stays the same.

(iii) The coding tiles $F_\perp, G_\perp$ and their positions in $V_\perp$ coincide for both tilings. The centre positions of the D-clusters of the two tilings must coincide. Inside the Delone clusters, the tetrahedra $(F^*_\parallel, G^*_\parallel)(\mathcal{T}^*, D_6)$ sit exactly inside the corresponding rhombohedra $(F^*_\parallel, G^*_\parallel)(\mathcal{T}^*, P)$. The difference between the D^a and D^b-clusters is manifest in the even/odd selection of the tetrahedra from the rhombohedral vertices. The covering of the tiles by the Delone clusters is governed by the criterion proposition 13. The covering of the tile windows by windows for Delone clusters centred at the vertices of the windows is studied in [19]. The result is that parts of the tile windows remain uncovered by windows for Delone clusters. Therefore the Delone covering of the tiles must be incomplete. Since the Delone clusters in the tiling always cover full tiles, it follows that the uncovered parts of the tile windows consists of full tiles sitting outside Delone clusters.

This analysis implies that the incomplete covering of the tiling can be constructively augmented into a complete covering: The tiles sitting outside Delone clusters augment the incomplete covering as glue tiles. These glue tiles have well defined windows. The corresponding construction is presently under study [18].

14. Conclusion

We show that Delone clusters with asymmetric fillings are general structures on dual projected tilings and have well defined windows. We define a fundamental domain for functions compatible with these tilings. We distinguish vertex and tile covering and give criteria for both in terms of windows. For the planar Penrose and triangle tiling, we have shown in [16, 17] that Voronoi and Delone clusters have unique filling properties, cover the tiling, form fundamental domains and appear in definite local configurations. The present Delone clusters in icosahedral three-dimensional tilings $(\mathcal{T}^*, P/D_6)$ display a more complex pattern: the icosahedral Delone clusters again have a unique and asymmetric filling. They cover the vertex points up to 98.7 per cent. This means that the Delone clusters organize the vertex points to a high degree.

Nevertheless these clusters do not cover all the tiles of the tiling. Glue tiles can fill the gaps between them. The fundamental domain property of the Delone clusters holds for the tiling $(\mathcal{T}^*, P)$, but does not hold for the tiling $(\mathcal{T}^*, D_6)$.

Problems for future study in these icosahedral tilings are the details of the closing of the gaps between Delone clusters by glue tiles, and the classification of local cluster configurations in a way similar to what was done for the triangle tiling in [17].

Acknowledgments

The author is grateful to Zorka Papadopolos and Gerald Kasner for many discussions on the geometry of icosahedral tilings, their windows and covering.

References

[1] Arnold V I 1988 Remarks on quasicrystal symmetry *Physica* D **33** 21–5
[2] Bohr H 1927 Beiträge zur Theorie der fastperiodischen Funktionen I *Math. Ann.* **96** 119–47
Bohr H 1927 Beiträge zur Theorie der fastperiodischen Funktionen II *Math. Ann.* **96** 383–406
[3] Conway J H and Sloane N J A 1988 *Sphere Packings, Lattices and Groups* (New York: Springer) pp 31–6
[4] Duneau M 1995 Quasicrystals with a unique covering cluster *Proc. 5th Int. Conf. on Quasicrystals (Avignon, 1995)* ed Ch Janot and R Mosseri (Singapore: World Scientific) pp 116–9
[5] Duneau M 2000 Clusters in quasicrystals *Proc. 7th Int. Conf. Quasicrystals (Stuttgart, 1999)* ed F Gaehler, P Kramer, H-R Trebin and K Urban *Mater. Sci. Eng.* A **294–296** 192–8
[6] Gratias, Puyraimond F, Quiquandon M and Katz A 2000 Atomic clusters in icosahedral F-type quasicrystals *Preprint*
[7] Gummelt P 1996 Penrose tilings as coverings of congruent decagons *Geometriae Dedicata* **62** 1–17
[8] Kepler J 1941 Strena seu de Nive Sexangula (1611) *Ges. Werke* vol 4, ed M Caspar and F Hammer (Munich) pp 259–80
[9] Katz A and Gratias D 1993 A geometric approach to chemical ordering in icosahedral structures *J. Non-Cryst. Solids* **153, 154** 187–95
[10] Katz A and Gratias D 1995 Chemical order and local configurations in AlCuFe-type icosahedral phase *Proc. Int. Conf. on Quasicrystals* ed C Janot and R Mosseri (Singapore: World Scientific) pp 164–7
[11] Kramer P 1987 Atomic order in quasicrystals is supported by several unit cells *Mod. Phys. Lett.* B **1** 7–18
[12] Kramer P and Papadopolos Z 1995 Symmetry concepts for quasicrystals and noncommutative crystallography *Proc. ASI Aperiodic Long Range Order (Waterloo, 1995)* ed R V Moody (New York: Kluwer) pp 307–30
[13] Kramer P and Schlottmann M 1989 Dualization of Voronoi domains and klotz construction: a general method for the generation of proper space filling *J. Phys. A: Math. Gen.* **22** L1097–102
[14] Kramer P, Papadopolos Z and Zeidler D 1992 Concepts of symmetry in quasicrystals *AIP Conf. Proc.* vol 266, ed A Frank, T H Seligman and K B Wolf pp 179–200
[15] Kramer P 1999 Quasicrystals: atomic coverings and windows are dual projects *J. Phys. A: Math. Gen.* **32** 5781–93
[16] Kramer P 2000 The cover story: Fibonacci, Penrose, Kepler *Proc. 7th Int. Conf. on Quasicrystals (Stuttgart, 1999)* ed F Gaehler, P Kramer, H-R Trebin and K Urban *Mater. Sci. Eng.* A **294–296** 401–4
[17] Kramer P 2000 Delone clusters, covering and linkage in the quasiperiodic triangle tiling *J. Phys. A: Math. Gen.* **33** 7885–901
[18] Kramer P *et al* 2001 Covering presentation and colouring of dual canonical tilings, in preparation
[19] Papadopolos Z and Kasner G 2000 Delone covering of canonical tilings $\mathcal{T}^{*(D_6)}$ *Proc. Aperiodic 2000*
[20] Jeong H-C and Steinhardt P J 1997 Constructing Penrose-like tilings from a single prototile and the implications for quasicrystals *Phys. Rev.* B **55** 3520–32